

Measurement of the top pair invariant mass distribution at 7 TeV and search for new physics

S. Rappoccio for the CMS Collaboration
Johns Hopkins University, Baltimore, MD, USA

An overview of searches for new physics in the $t\bar{t}$ sample from the CMS Collaboration is presented with data collected at the Large Hadron Collider at $\sqrt{s} = 7$ TeV. There are several searches presented, including same-sign dilepton signatures, semileptonic signatures, and all-hadronic signatures, the latter of which uses advanced jet reconstruction techniques.

I. INTRODUCTION

A number of scenarios for physics beyond the Standard Model (BSM) feature new gauge interactions with favorable couplings to the third-generation quarks (for instance, see References [1–9]). These couplings result in new heavy states which could appear as resonances in top pair production at the LHC. For example, Reference [10] shows an example of these heavy states expressed as Kaluza-Klein gluons with concrete predictions of cross sections and branching ratios. Also of note are models that have recently been proposed to solve the discrepancy in the top pair production forward-backward asymmetry from the Tevatron (Reference [11–15]). For instance, one recent model-independent study of the implications of the forward-backward asymmetry is presented in Reference [16], which argues that a strong enhancement of the production cross section of $t\bar{t}$ pairs must be seen at the LHC for invariant masses above 1.5 or 2.0 TeV/ c^2 if the deviation is due to new physics at a heavy mass scale Λ .

Searches for new physics in top pair production have been performed by the Tevatron experiments [17–19]. The Tevatron measurements provide the most stringent lower mass limits for a narrow resonance, where a narrow topcolor leptophobic $t\bar{t}$ resonance is excluded for masses below about 800 GeV/ c^2 .

The results presented in this paper are based on data collected by the CMS experiment in 2010 and 2011 at a center-of-mass energy of 7 TeV, between 0.036 and 1.1 fb $^{-1}$. Full descriptions of these analyses are presented in References [20–23].

II. ALL HADRONIC DECAY CHANNEL

The all-hadronic analysis in Reference [20] utilizes 0.8 fb $^{-1}$ of data, and exploits the highly-boosted nature of the top quarks from the high-mass resonances, namely the fact that the top quark’s decay products often fall inside a single jet. If the boost is not too large, the decay products are distinguishable in this jet (in particular, the W boson decay products), and this information can be used to reduce the large generic QCD dijet production. These decay products within the jet are referred to as “subjets”.

A *top tagging algorithm* [24, 25] is used to identify merged top jets by analyzing their substructure. This is accomplished by examining the clustering sequence of the jets, and the application of specialized selection criteria. The behavior of jets from heavy particles such as top quarks is different from generic QCD jets. For instance, QCD jets tend to have very few subjets within them, whereas the jets that originate from hadronic top decays have three or four subjets. Furthermore, the kinematics of these subjets is different. While the subjets of generic QCD jets tend to be close together and one often dominates the jet energy (due to gluon emission in the final state), the top quark decay products share the jet energy more equally and emerge at wider angles.

The masses involved in the process (the top mass and the W mass) also give strong handles for such discrimination. The mass of a typical QCD jet exhibits a falling spectrum after a quick initial rise (Reference [26]), whereas the mass of a fully merged jet from a top quark is very close to the top mass (170-175 GeV/ c^2). It is often possible to identify two of the subjets within the top jet as coming from the decay of the W. Similarly to the mass of the entire jet, for generic QCD jets the mass of this W candidate has a falling spectrum in the region of interest, whereas the W decay products from the sequential top decay are very close to the W mass.

For situations where the decay products of the top quark are not contained entirely in one jet, a technique has also been developed to discriminate against QCD backgrounds using similar techniques as described for the fully-merged case. However, for this purpose a tool is deployed that is able to handle more general topologies than the “top jet tagger” targeted specifically at the hadronic top decays.

The *jet pruning algorithm*, presented in Reference [27, 28], can be used to identify substructure from general topologies. While this tool has been shown to be slightly less performant on fully boosted top jets than

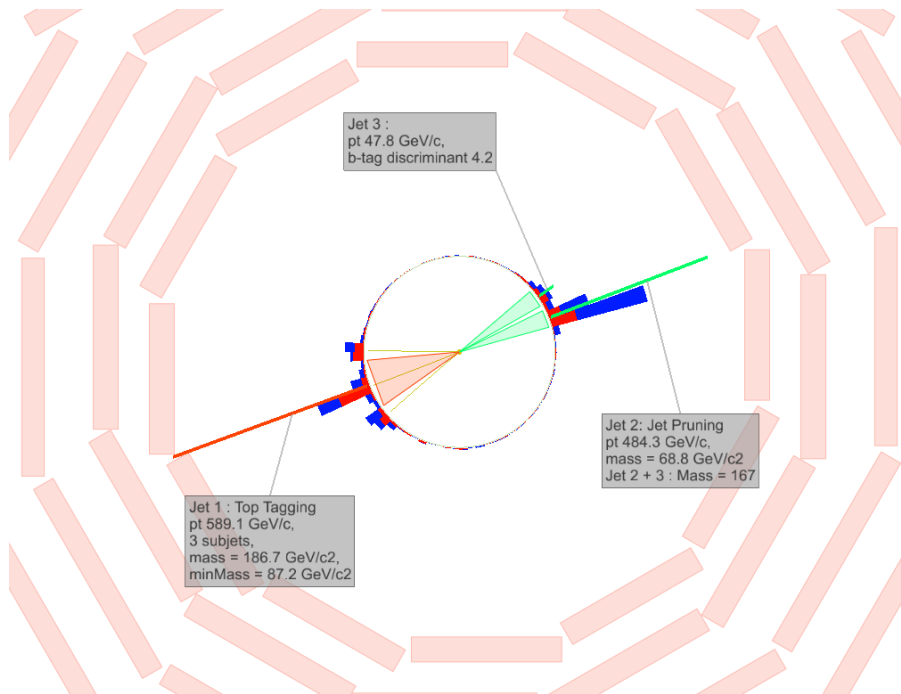


FIG. 1: Event display of a “golden” triply-tagged all-hadronic $t\bar{t}$ candidate. The invariant mass of the $t\bar{t}$ candidate is $1352.5 \text{ GeV}/c^2$. This event has a requirement of a top-tagged jet (orange, with yellow subjets), a W-tagged jet and a bottom-tagged jet (both shown in green). The electromagnetic calorimeter information is shown in red, and the hadronic calorimeter information is shown in blue.

the targeted top jet tagger, it is of more general utility for arbitrary topologies. Reference [29] has detailed algorithmic comparisons of the taggers for fully boosted top systems, and for instance, for the same efficiency to identify true top quarks, the probability to misidentify a generic QCD jet with the jet pruning algorithm is larger by 20-30% than the targeted top jet tagger.

On the other hand, the targeted top tagging tool is not immediately applicable to moderately boosted top quark systems where not all of the decay products are merged, and as such, the jet pruning tool is used to develop an algorithm that identifies boosted hadronically-decaying W-bosons into one jet (referred to as a W jet). In this case, the fact that the decay products from generic QCD jets are radiated fairly asymmetrically is exploited, whereas the decay products from the W are more symmetric because they arise from a two-body decay of W boson. Top quark candidates are then constructed by combining this W jet with another jet that is close to it, and form a full top-quark candidate.

Figure 1 shows an event display of a “golden” triply-tagged all-hadronic $t\bar{t}$ candidate. The event contains a top-tagged jet, a W-tagged jet, and a bottom-tagged jet. This is a sample that has an enhanced $t\bar{t}$ contribution.

A demonstration of the ability to extract boosted jets in a well-controlled high purity subsample of the data is shown in Figures 2 and 3. In these figures, a sample of moderately boosted top quarks is extracted from the semileptonic decay channel by requiring strong transverse momentum cuts to hemispherically separate the top quark decay products. The mass of the highest mass jet in the “hadronic” hemisphere is shown (corresponding to the W mass), as well as the invariant mass of the W candidate with the nearest jet, which is the mass of the top quark candidate. This is a very pure $t\bar{t}$ sample with negligible backgrounds, and the data are well-reproduced by the Monte Carlo expectations. The W peak is quite pronounced, and demonstrates the efficacy of the methodology in extracting massive boosted hadronic final states using substructure techniques.

From this sample, the subjet jet energy scale can be determined from the difference in the W mass peaks in data and Monte Carlo. The subjet energy scale is measured to be 1.01 ± 0.04 given this sample. In addition, the efficiency to select W candidate jets can be measured in the same sample by comparing the event selection efficiency in data and Monte Carlo, and assuming that the same ratio (or “scale factor”) applies to other samples. The data-to-Monte-Carlo scale factor is determined to be 0.93 ± 0.13 .

In Reference [20] there are actually two analyses, one in the dijet topology (utilizing two top tags), and one in the trijet topology (utilizing one top tag and one W-tag). The results are combined for a final limit.

The background estimates for both analyses are taken primarily from data. The small contribution from

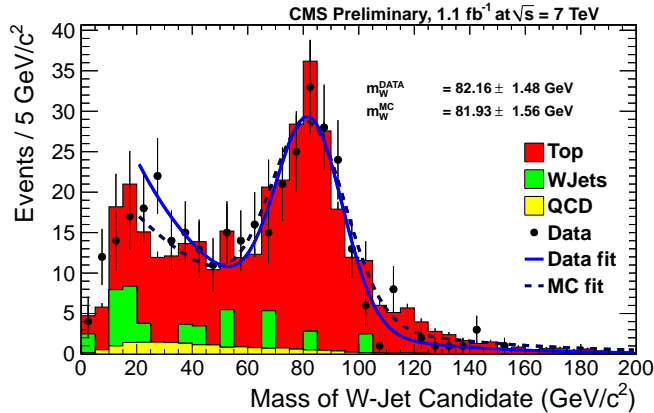


FIG. 2: Mass of the highest mass jet in a semileptonic top sample.

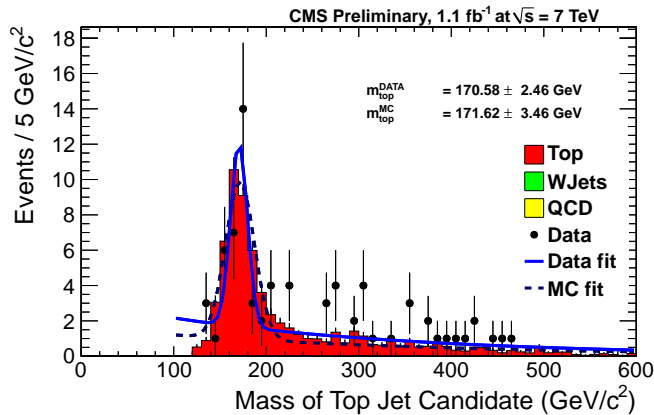


FIG. 3: Mass of the hadronic top candidate in a semileptonic top sample.

Standard Model $t\bar{t}$ decays is taken from Monte Carlo, correcting for trigger efficiency, the efficiency of the top- and W-tagging algorithms, and jet energy scale. The largest background, however, is generic QCD production which has been mis-identified as having substructure (“mistags”). This background is estimated by weighting jets in a sample before applying the final top-jet tag, where the weighting factor is derived from generic dijet data that has been signal depleted.

Figure 4 shows the results of the event selection in the dijet topology (similar plots for the trijet topology can be seen in the original reference). Extremely good agreement is observed with the prediction, and hence a limit on new physics models is formulated. The technique chosen is to hypothesize a counting experiment in a signal window (chosen by the expected size of a narrow resonance in the $t\bar{t}$ invariant mass spectrum). A Bayesian technique is chosen to represent the limits on new physics models, with Jeffreys priors on the cross section of new physics, and log-normal priors on the nuisance parameters. The dijet and trijet topologies are combined in a final exclusion calculation shown in Figure 5, which shows the 68% and 95% credible intervals for observing a resonance at a given mass with a given cross section times branching ratio. Several theoretical models are also included for comparison.

III. SEMILEPTONIC DECAY CHANNEL

There are two analyses from CMS in the semileptonic decay channel. The first analysis (Reference [21], with 0.036 fb^{-1}) utilizes standard event reconstruction techniques assuming that the top quark’s decay products are isotropically distributed (i.e. close to production threshold). The events are required to have at least three

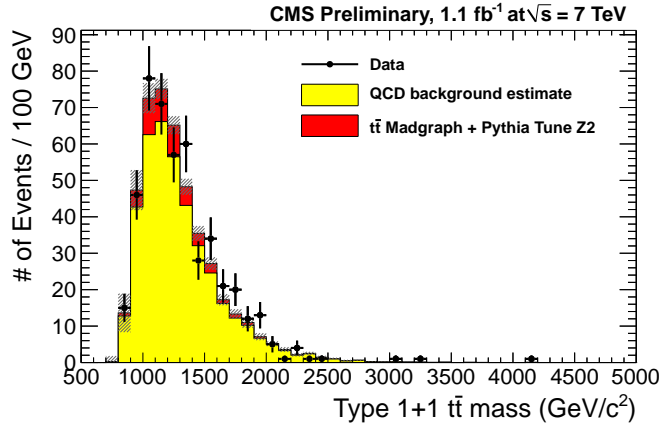


FIG. 4: Results of the all-hadronic analysis in the dijet topology. The yellow histogram is the QCD estimate from the data-driven technique described in the text, and the red histogram is the estimate from $t\bar{t}$ continuum production. The black points are the data. The shaded gray boxes indicate the statistical and systematic uncertainty on the total background estimate.

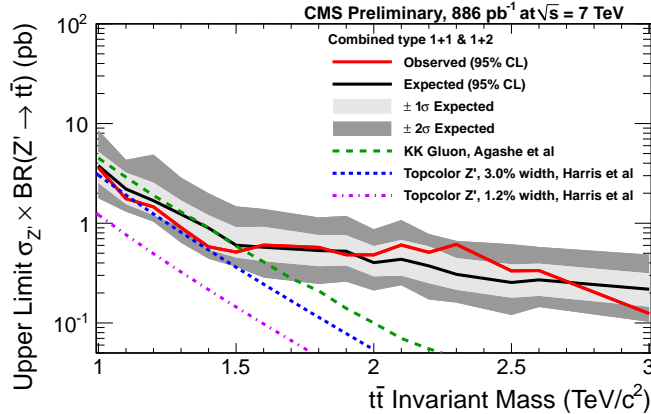


FIG. 5: The 95% C.L. upper limit on a product of the production cross section of the $t\bar{t}$ invariant mass and a branching fraction for its decay into $t\bar{t}$ pair, as a function of assumed mass. Three theoretical models are examined in shades of purple. From top to bottom: a Kaluza-Klein gluon from Reference [10], updated to 7 TeV via private communication with the authors (Note: the KK gluon model has a width larger than that of the signal Monte Carlo); a topcolor Z' model from Reference [30] with width 3%; and a topcolor Z' model from Reference [30] with width 1.2%.

jets, one well-isolated muon or electron, and significant missing transverse energy. The events are categorized according to the lepton type (muon or electron), the number of jets, and the number of tags in the event, which are then linked by the expected jet energy scale and bottom-quark tagging efficiency. This technique is similar to that in the recent measurement of the top pair production cross section in Reference [31] (recently updated to 1 fb^{-1} in Reference [32]).

The $t\bar{t}$ candidate is constructed by assigning jets to partons with a χ^2 sorting method. The combination with the smallest χ^2 is selected as the best candidate. The top-quark and W-boson masses are used in the constraints of the χ^2 sorting method, and to solve the quadratic ambiguity of the z -component of the neutrino's four-vector.

The backgrounds are primarily taken from Monte Carlo simulations comparably to that described in Reference [31]. The non-prompt-W backgrounds are taken from data, in sidebands of the missing transverse energy and isolation selection criteria with a two-dimensional extrapolation.

Figures 6 and 7 show the results of the event selection for two of the eight subsamples of the data. Here are shown the muon subsample with at least four jets and exactly zero bottom-quark-tagged jets, and the muon

subsample with exactly three jets and at least two bottom-quark-tagged jets. Good agreement between the data and expectation is observed, and hence a limit is set on possible new physics models.

In order to evaluate the statistical limits, a shape analysis is performed on the $t\bar{t}$ invariant mass spectrum. A fully Bayesian approach is taken, as in the all-hadronic case. The same prior distributions are chosen as well. Figure 8 shows the limits on the production cross section times branching ratio of a $t\bar{t}$ resonance at a given mass. Good agreement with the data is observed.

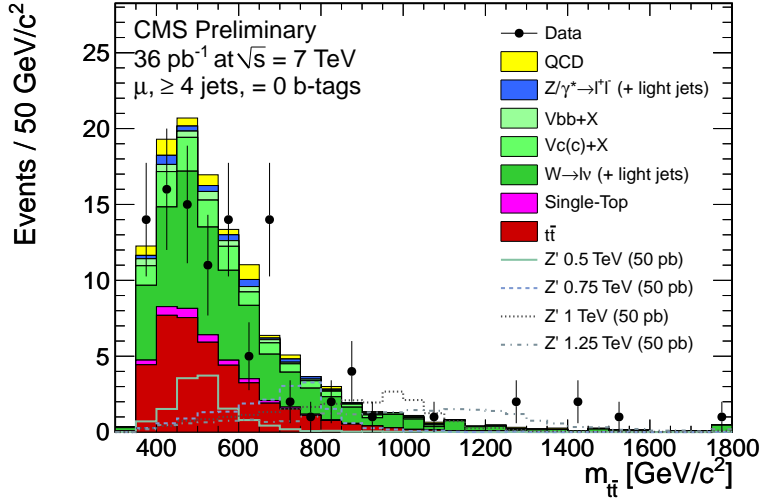


FIG. 6: Results of event selection for the first semileptonic analysis which assumes an isotropically decaying $t\bar{t}$ candidate. The bin shown here is the subsample of data with at least four jets and exactly zero bottom-quark-tagged jets.

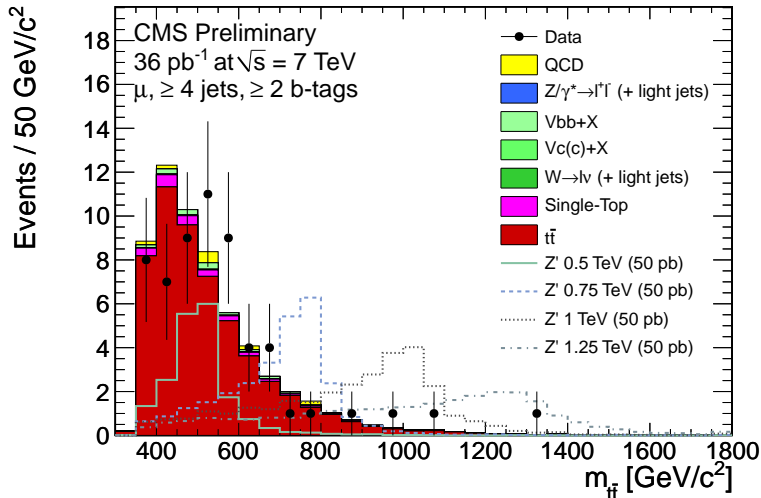


FIG. 7: Results of event selection for the first semileptonic analysis which assumes an isotropically decaying $t\bar{t}$ candidate. The bin shown here is the subsample of data with exactly three jets and at least two bottom-quark-tagged jets.

The second analysis (Reference [22], with 1.1 fb^{-1}) assumes a boosted topology and modifies the event selection criteria in order to efficiently reconstruct the top quarks in this regime. The number of required jets must be reduced because there is significant jet merging. The isolation criteria on the muon must also be modified because the boost of the top quark merges the muon with the nearby bottom-quark jet.

Instead of the traditional isolation criterion, a new criterion is applied in this analysis, which selects events with a two-dimensional distribution. The first dimension is the angular separation between the muon and the nearest jet (ΔR_{min}). The second dimension is the transverse momentum of the leading jet relative to the muon (p_T^{REL}). Events fail the selection if they have $\Delta R_{min} < 0.5$ and $p_T^{REL} < 25 \text{ GeV}/c$. Furthermore, non-prompt-

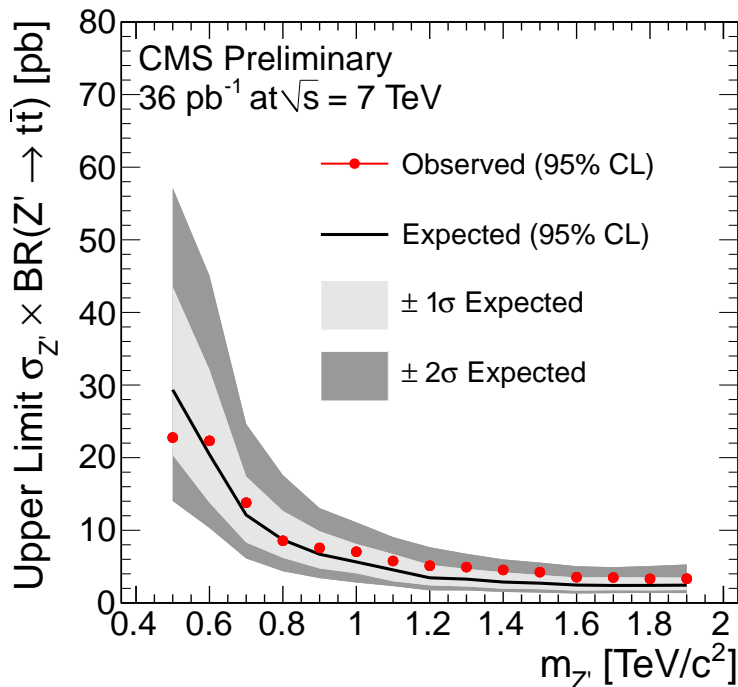


FIG. 8: The 95% C.L. upper limit on a product of the production cross section of the $t\bar{t}$ invariant mass and a branching fraction for its decay into $t\bar{t}$ pair, as a function of assumed mass. This is for the first semileptonic analysis which assumes an isotropically decaying $t\bar{t}$ candidate.

W-boson backgrounds are suppressed by requiring that the scalar sum of the lepton transverse momentum and the missing transverse energy ($H_{T,lep}$) be larger than 150 GeV/ c^2 . The region with $H_{T,lep}$ smaller than 150 GeV/ c^2 is used to normalize the residual non-prompt-W-boson backgrounds.

The remaining backgrounds are taken from Monte Carlo as in the case of the first semileptonic analysis. However, in this analysis no bottom-quark-tagging information is used. Figure 9 shows the results of the event selection in this boosted analysis, and Figure 10 shows the 68% and 95% credible intervals for observing a resonance at a given mass with a given cross section times branching ratio. Several theoretical models are also included for comparison. The same mathematical formalism is used as in the first semileptonic analysis.

IV. FULLY LEPTONIC DECAY CHANNEL

The fully leptonic analysis is a search for anomalous same-sign dilepton events with 0.036 fb^{-1} . It is a reinterpretation of a SUSY search (Reference [33]). This search is reinterpreted as a search in the top sector to examine the hypothesis put forward in Reference [34] to explain the top forward-backward asymmetry observed at the Tevatron. In that paper, the forward-backward asymmetry of top-pair production is enhanced by the presence of a flavor-changing-neutral-current Z' interaction which can then produce same-sign top events.

To test this model, the analysis in the dilepton channel requires two positive leptons, two or more jets, and missing transverse energy. The analysis is a counting experiment, with 0.9 ± 0.6 events expected from the Standard Model, and 2 events observed. With this data, limits on the FCNC Z' models can be placed based on the mass of the boson and the right-handed coupling (f_R).

Figure 11 shows the 95% confidence level limit on the model, with varied boson masses and right-handed couplings. The model proposed by Reference [34] is disfavored.

A. Conclusions

In conclusion, new physics in the top sector is being rigorously pursued at CMS with a variety of reconstruction techniques, including recent advances in boosted jet reconstruction. The plausible new physics scenarios to

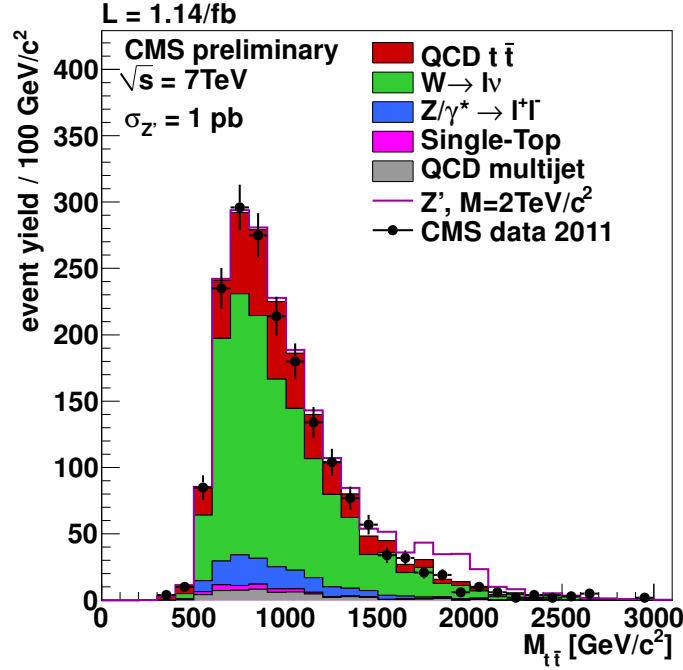


FIG. 9: Results of event selection for the second semileptonic analysis which assumes a boosted $t\bar{t}$ candidate.

explain the top forward-backward asymmetry anomaly at the Tevatron are beginning to be eliminated, and future studies will help to further elucidate the situation.

-
- [1] S. Dimopoulos and H. Georgi, Nucl. Phys. **B193**, 150 (1981).
 - [2] S. Weinberg, Phys. Rev. **D13**, 974 (1976).
 - [3] L. Susskind, Phys. Rev. **D20**, 2619 (1979).
 - [4] C. T. Hill and S. J. Parke, Phys. Rev. **D49**, 4454 (1994), hep-ph/9312324.
 - [5] R. S. Chivukula, B. A. Dobrescu, H. Georgi, and C. T. Hill, Phys. Rev. **D59**, 075003 (1999), hep-ph/9809470.
 - [6] N. Arkani-Hamed, A. G. Cohen, and H. Georgi, Phys. Lett. **B513**, 232 (2001), hep-ph/0105239.
 - [7] N. Arkani-Hamed, S. Dimopoulos, and G. R. Dvali, Phys. Lett. **B429**, 263 (1998), hep-ph/9803315.
 - [8] L. Randall and R. Sundrum, Phys. Rev. Lett. **83**, 3370 (1999), hep-ph/9905221.
 - [9] L. Randall and R. Sundrum, Phys. Rev. Lett. **83**, 4690 (1999), hep-th/9906064.
 - [10] K. Agashe, A. Belyaev, T. Krupovnickas, G. Perez, and J. Virzi, Phys. Rev. **D77**, 015003 (2008), hep-ph/0612015.
 - [11] T. Aaltonen et al. (CDF), Phys. Rev. Lett. **101**, 202001 (2008), 0806.2472.
 - [12] V. M. Abazov et al. (D0), Phys. Rev. Lett. **100**, 142002 (2008), 0712.0851.
 - [13] T. Aaltonen et al. (CDF), Phys. Rev. **D83**, 112003 (2011), 1101.0034.
 - [14] D0 Note **6062-CONF** (2010).
 - [15] CDF Note **10436** (2011).
 - [16] C. Delaunay, O. Gedalia, Y. Hochberg, G. Perez, and Y. Soreq, JHEP **1108**, 031 (2011), 1103.2297.
 - [17] T. Aaltonen et al. (CDF), Phys. Rev. **D77**, 051102 (2008), 0710.5335.
 - [18] T. Aaltonen et al. (CDF), Phys. Rev. Lett. **100**, 231801 (2008), 0709.0705.
 - [19] D0 Note **5882-CONF** (2009).
 - [20] CMS PAS EXO-11-006 (2011), URL <http://cdsweb.cern.ch/record/1370237/>.
 - [21] CMS PAS TOP-10-007 (2010), URL <http://cdsweb.cern.ch/record/1335720/>.
 - [22] CMS PAS EXO-11-055 (2011), URL <http://cdsweb.cern.ch/record/1376673/>.
 - [23] S. Chatrchyan et al. (CMS Collaboration), JHEP **1108**, 005 (2011), * Temporary entry *, 1106.2142.
 - [24] D. E. Kaplan, K. Rehermann, M. D. Schwartz, and B. Tweedie, Phys. Rev. Lett. **101**, 142001 (2008), 0806.0848.
 - [25] CMS PAS JME-009-01 (2009), URL <http://cdsweb.cern.ch/record/1194489/>.

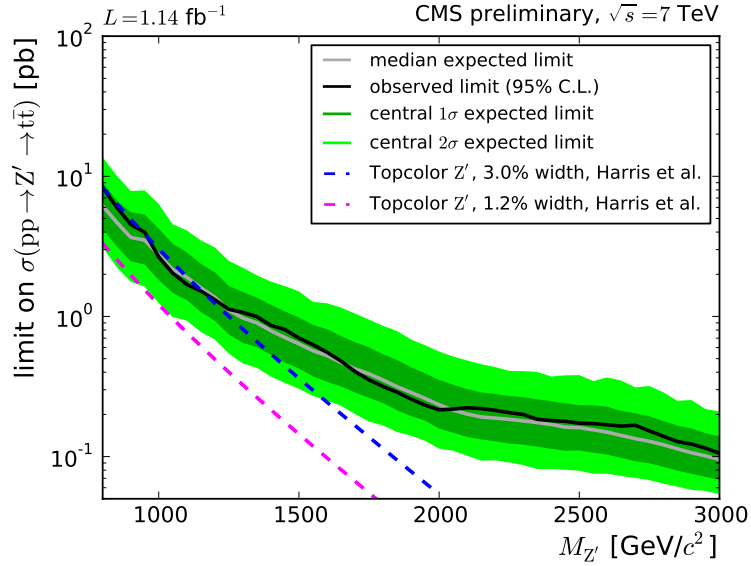


FIG. 10: The 95% C.L. upper limit on a product of the production cross section of the $t\bar{t}$ invariant mass and a branching fraction for its decay into $t\bar{t}$ pair, as a function of assumed mass. This is for the second semileptonic analysis which assumes a boosted $t\bar{t}$ candidate.

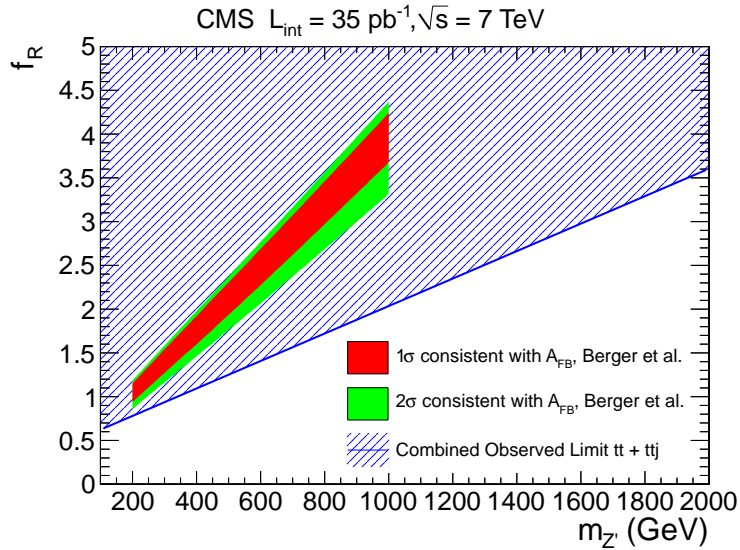


FIG. 11: The 95% C.L. upper limit on the model proposed by Reference [34] as a function of the boson mass and the right-handed coupling parameter f_R . The model is disfavored by the CMS data.

- [26] S. D. Ellis, J. Huston, K. Hatakeyama, P. Loch, and M. Tonnesmann, *Prog. Part. Nucl. Phys.* **60**, 484 (2008), 0712.2447.
- [27] S. D. Ellis, C. K. Vermilion, and J. R. Walsh, *Phys.Rev.* **D80**, 051501 (2009), 0903.5081.
- [28] S. D. Ellis, C. K. Vermilion, and J. R. Walsh, *Phys.Rev.* **D81**, 094023 (2010), 0912.0033.
- [29] A. Abdesselam, E. Kuutmann, U. Bitenc, G. Brooijmans, J. Butterworth, et al., *Eur.Phys.J.* **C71**, 1661 (2011), 1012.5412.
- [30] R. M. Harris, C. T. Hill, and S. J. Parke (1999), hep-ph/9911288.
- [31] S. Chatrchyan et al. (CMS Collaboration) (2011), 1108.3773.
- [32] CMS PAS TOP-11-003 (2011).
- [33] S. Chatrchyan et al. (CMS Collaboration), *JHEP* **1106**, 077 (2011), 1104.3168.
- [34] E. L. Berger, Q.-H. Cao, C.-R. Chen, C. S. Li, and H. Zhang, *Phys.Rev.Lett.* **106**, 201801 (2011), 1101.5625.